

Low energy Ar^+ ion beam induced kinetic roughening of thin Pt films on a Si substrate

P. Karmakar and D. Ghose*

*Saha Institute of Nuclear Physics,
Sector - I, Block - AF, Bidhan Nagar, Kolkata 700064, India*

October 25, 2018

Abstract

A 30 nm Pt thin film evaporated onto a Si wafer was sputtered by 8 keV Ar^+ ions at various ion doses. The evolution of the modified sputtered films was monitored by atomic force microscopy (AFM), high resolution scanning electron microscopy (HRSEM) and Rutherford backscattering spectrometry (RBS). The most interesting observation was the formation of mound-like structures on the metal surface. Morphological data were quantitatively analysed within the framework of the dynamic scaling theory. Analyses of the height-height correlation function for different doses yield roughness exponents α in the range 0.65 - 0.87, while the root-mean-square roughness amplitude w evolves with the dose ϕ as a power law $w \propto \phi^\beta$, with the growth exponent, $\beta \approx 0.3$. The results are discussed.

PACS numbers: 68.35.Ct, 79.20.Rf, 61.80.Jh

*Corresponding author. e-mail: ghose@surf.saha.ernet.in

I. INTRODUCTION

Low energy ion beam (typically 1 - 10 keV) sputtering is commonly used in most of the analytical depth-profiling techniques including secondary ion mass spectrometry (SIMS) and Auger electron spectroscopy (AES). Also, low energy ion beam system forms an essential part in various surface processing techniques such as ion beam etching, deposition and ion beam assisted growth. During the bombardment process, the interaction between the projectile ion and the target atoms lead to different phenomena, e.g., the topographical modification of the sample surface. A large variety of characteristic surface structures ranging from stochastic rough surface to the formation of well-defined conical protrusions [1, 2] are found to develop on the sputtered surfaces. Recently, there is a growing interest for the fabrication of sputtering induced surface structures in the submicron length scale because of possible technological applications [3]. Different scaling theories for the evolution of the surface roughness have been proposed [4] in order to understand the underlying physical processes involved and eventually determining a way of optimising control of the process.

In this paper, we have investigated the development of ion beam sputtering-induced surface morphologies in thin Pt films evaporated onto Si substrates. The analyses of the irradiated samples were done by atomic force microscopy (AFM), high resolution scanning electron microscopy (HRSEM) and Rutherford backscattering spectrometry (RBS).

II. EXPERIMENTAL

Thin Pt films ($\simeq 30$ nm) were deposited by d. c. magnetron sputtering onto commercially available polished Si (100) wafers, previously degreased and cleaned. The base pressure in the deposition chamber was 2×10^{-6} mbar. The Pt/Si samples were then sputtered with 8 keV Ar^+ ions at different doses in a low energy ion beam set-up developed in the laboratory [5]. The angle of ion incidence with respect to the surface normal was 45° . The average current density was $10 \mu\text{A}/\text{cm}^2$. The ion dose was measured by a current integrator (Danfysik, model 554) after suppression of the secondary electrons. The samples were exposed to total ion doses between 1×10^{15} and 2×10^{18} ions/cm². The base pressure in the target chamber was less than 5×10^{-8} mbar. The surface morphology of the ion-irradiated samples was examined by a Park Scientific AFM (Auto Probe CP) as well as by a high resolution scanning electron microscope (Hitachi S-4700) operated at 15 kV and viewed at 20° . Compositional profiles in the samples were analyzed by means of Rutherford backscattering of 2 MeV He^{2+} ions with the scattering angle set at 110° .

III. RESULTS AND DISCUSSION

Atomic force microscopy of the initial Pt surface topography shows a smooth continuous film with a root-mean-square (rms) roughness $w \simeq 0.2 \text{ nm}$. Fig. 1 shows the AFM images from the sample surfaces sputtered at successive increasing ion doses ϕ (different bombarding times t). Immediately after the start of the bombardment mound-like or globular structures begin to appear. The bombardment also produces voids or vacant regions in between the mounds. Both the lateral size and the height of the mounds become larger with increasing ion dose upto $\sim 10^{17} \text{ ions/cm}^2$; thereafter the sizes tend to decrease rapidly as the sputtering further continues. In the fluence region $10^{16} \text{ ions/cm}^2$ the mounds are quite sharp and well developed. However, at doses $\geq 2 \times 10^{16} \text{ ions/cm}^2$, the mounds tend to form clusters and become blurred. In a separate experiment we have bombarded a clean Si (100) wafer under identical conditions at various doses upto $10^{19} \text{ ions/cm}^2$. But in no case we find development of any surface structure in the virgin Si surface within the present AFM resolution, as also reported by Vajo et al. [6]. Therefore, it appears that the observed morphological structures are the characteristics of the Pt films. The sputtered surface topography was also investigated simultaneously using HRSEM. Although the image resolution and contrast are not as good as that of AFM, the results also show similar topographical evolution. For comparison typical HRSEM images at two different ion doses are shown in Fig. 2. Finally, comparison of the RBS spectra of the as-deposited sample and the ion-irradiated samples show that both the height and the width of the Pt profile reduce gradually due to ion beam sputtering, while the implanted Ar peak tends to develop as the bombardment is continued (Fig. 3). Energy dispersive x-ray analysis of the irradiated samples carried out in HRSEM also confirms the erosion of Pt due to Ar^+ bombardment.

In order to quantitatively characterize the observed morphology, we have studied the scaling properties of the interface. Family and Vicsek [7] analyzed the behavior of growing surfaces by assuming that they were self-affine such that the root-mean-square (rms) roughness or the interface width, $w(t)$ obeys the relation:

$$w(L, t) = L^\alpha f(t/L^z), \quad (1)$$

where L is the length scale over which the roughness is measured and t is the elapsed time of growth. The scaling function $f(u)$ behaves as u^β for $u \ll 1$ and as a constant for $u \gg 1$. The two parameters α and β are called the static (or spatial) and dynamic (or temporal) scaling exponents, respectively, and z is equal to α/β . A standard method for investigating surface morphology is to study the height-height correlation function $G(\mathbf{r}, t)$, which is the mean square of height difference between two surface positions separated by a lateral distance \mathbf{r} :

$$G(\mathbf{r}, t) = \langle [h(\mathbf{r}, t) - h(0, t)]^2 \rangle. \quad (2)$$

If the surface is scale invariant and isotropic, then $G(\mathbf{r}, t)$ has the following properties:

$$G(r, t) \sim \begin{cases} r^{2\alpha} & \text{for } r \ll \xi(t) \\ 2w^2(t) & \text{for } r \gg \xi(t) \end{cases}, \quad (3)$$

where $\xi(t)$ is the lateral correlation length which scales as $t^{1/z}$. $w(t)$ is given by:

$$w(t) = \sqrt{\langle [h(\mathbf{r}, t) - \langle h \rangle]^2 \rangle} \propto t^\beta, \quad (4)$$

where $\langle \dots \rangle$ denotes the spatial average over the sample surface. The width function provides a measure of the vertical height fluctuation of the surface profile at different bombardment times t ($\propto \phi$).

In the present case the correlation function (Eq. (2)) was evaluated directly from the AFM micrographs by taking every possible pair of positions, calculating the square of the height difference and averaging for equal distances. Shown in Fig. 4 are the typical log-log plot of $G(r, t)$ vs lateral distance r at three different bombarding ion doses, ϕ . From the figure it is seen that $G(r, t)$ increases linearly at small r following a plateau at large r , consistent with the asymptotic behavior predicted in Eq. (3). The lateral position corresponding to the plateau point is equal to ξ , which is a representative measure of the average dimension of the mound. The roughness exponent α was determined by least-squares fitting to the linear slope of $G(r, t)$ at small r . In the dose range investigated here we observed α in the range 0.65 - 0.87 (Fig. 5). The rms roughness or the interface width w at each time (or dose) was obtained from the in-built software of the AFM instrument and it was found that they all agree to those calculated from the asymptotic value of $G(r, t)$ for $r \gg \xi(t)$ as stated in Eq. (3). These data of w versus ion dose in a log-log plot are shown in Fig. 6. It is interesting to note that after a certain bombarding dose when the film material is eroded enough away, the rms surface roughness values show a sharp fall. The exponent β was determined from the linear fit of the ascending part of the roughness curve and is found to be about 0.3. Fig. 7 shows a power law increment of the correlation length ξ with increasing ion dose ϕ , as expected, with the dynamic exponent $1/z \approx 0.39$.

The evolution of surface morphology is thought to govern by the interplay and competition between the dynamics of surface roughening on the one hand and material transport during surface diffusion on the other. Various stochastic nonlinear continuum models have been introduced to explain the temporal and spatial evolution of surface morphologies [8]. One such formalism is the noisy Kuramoto-Sivashinsky (KS) equation [9] which is believed to encompass most of the roughening and smoothing processes that are occurred during ion beam sputtering of surfaces. The KS equation describes the temporal evolution of surface height function h as

$$\frac{\partial h}{\partial t} = \nu \nabla^2 h - \kappa \nabla^4 h + \frac{\lambda}{2} |\nabla h|^2 + \eta, \quad (5)$$

where ν is the "negative surface tension" generated by the erosion process, κ is the coefficient of thermal or ion induced surface diffusion, λ is a nonlinear coefficient attributed to the tilt-dependent erosion rate, and η is the noise term which accounts the randomness in the arrival of the bombarding ions. This equation was solved numerically in 2+1 dimensions [9], which yields the scaling exponents $\alpha = 0.75 - 0.8$, $\beta = 0.22 - 0.25$ and $z = 3.0 - 4.0$, respectively. The exponents which are observed in the present experiment nearly correspond to the above predicted values. It is interesting to mention here that the present results are also consistent to the scaling laws obtained in the experiment of sputter-deposition growth of Pt by Jeffries et al. [10]. This supports the assumption often made that the sputter erosion is equivalent to the inverse of the growth process [4]. The development of observed structures may be explained by the so-called "ion-induced grain growth" as proposed by Hasegawa et al. [11], where it is thought that surface diffusion causes the adatoms to migrate preferentially to those grains which are at energetically favored orientations [12]. Consequently, these grains tend to grow with time and are transformed eventually to mounds due to minimization of surface free energy. For thin films, one should consider a further effect of ion beam responsible for the decay of kinetic roughening at the later stages of bombardment, namely, the loss of material due to sputter erosion from the sample. After prolonged bombardment, when the film is thin enough the particle supply through surface diffusion is supposed to no longer compete with the sputter removal of atoms as a result of which the mounds cease to grow and ultimately disappear. For relatively thick metal films, the growth process continues and the mounds are finally transformed by further erosion to sharp conical structures [13]. The high α value is an indicative of higher rate of surface diffusion compared to that of sputtering which is necessary for the growth and/ or stabilization of the surface structures.

ACKNOWLEDGMENTS

The authors thank Dr. S. Kundu for the preparation of the Pt thin films, Mr. A. Das for technical assistance during the AFM measurements and to IOP, Bhubaneswar for RBS measurements. Finally, the authors are grateful to Prof. F. Okuyama of Nagoya Institute of Technology for HRSEM measurements.

References

- [1] *Beam Effects, Surface Topography and Depth Profiling in Surface Analysis*, Eds. A. W. Czanderna, T. E. Madey and C. J. Powell (Plenum Press, New York, 1998).
- [2] D. Ghose and S. B. Karmohapatro, in: *Advances in Electronics and Electron Physics*, Ed. P. Hawak (Academic Press, New York, 1990), Vol. 79, p. 73.
- [3] S. Facsko, T. Dekorsy, C. Koerdt, C. Trappe, H. Kurz, A. Vogt, and H. L. Hartnagel, *Science* **285**, 1551 (1999).
- [4] A. -L. Barabási and H. E. Stanley, *Fractal Concepts in Surface Growth* (Cambridge University Press, Cambridge, England, 1995).
- [5] P. Karmakar, P. Agarwal and D. Ghose, *Appl. Surf. Sci.* 178 (2001) 83.
- [6] J. J. Vajo, R. E. Doty, and E. -H. Cirlin, *J. Vac. Sci. Technol. A* **14** (1996) 2709.
- [7] F. Family and T. Vicsek, *Dynamics of Fractal Surfaces* (World Scientific, Singapore, 1991).
- [8] R. Cuerno and A. -L. Barabási, *Phys. Rev. Lett.* **74**, 4746 (1995).
- [9] J. T. Drotar, Y. -P. Zhao, T. -M. Lu, and G. -C. Wang, *Phys. Rev. E* **59**, 177 (1999).
- [10] J. H. Jeffries, J. -K. Zuo and M. M. Craig, *Phys. Rev. Lett.* **76**, 4931 (1996).
- [11] Y. Hasegawa, Y. Fujimoto and F. Okuyama, *Surf. Sci.* 163 (1985) L781.
- [12] S. Rusponi, G. Costantini, F. Buatier de Mongeot, C. Boragno, and U. Valbusa, *Appl. Phys. Lett.* **75**, 3318 (1999).
- [13] M. Tanemura and F. Okuyama, *Nucl. Instrum. Methods B47* (1990) 126.

Figure captions

Fig. 1. Some selected AFM images of Ar^+ sputtered Pt/Si surfaces, showing a sequence of the evolution of the surface topography with increasing ion doses: (a) $2 \times 10^{15} \text{ ions/cm}^2$; (b) $7 \times 10^{15} \text{ ions/cm}^2$; (c) $2 \times 10^{16} \text{ ions/cm}^2$; (d) $5 \times 10^{16} \text{ ions/cm}^2$; (e) $7 \times 10^{16} \text{ ions/cm}^2$ and (f) $2 \times 10^{17} \text{ ions/cm}^2$.

Fig. 2. Typical scanning electron micrographs of Ar^+ sputtered Pt/Si surfaces at ion doses (a) $7 \times 10^{15} \text{ ions/cm}^2$ and (b) $2 \times 10^{16} \text{ ions/cm}^2$.

Fig. 3. Pt distribution of RBS spectra for Pt/Si at 8 keV Ar^+ ion beam sputtering as a function of ion dose.

Fig. 4. Some typical log-log plots of the height-height correlation functions $G(r, t)$, calculated from AFM images, as a function of the lateral distance r for different bombarding doses ϕ as indicated.

Fig. 5. The plot of the roughness exponent α versus ion dose ϕ .

Fig. 6. Showing the rms surface roughness w vs the bombarding ion dose ϕ . The solid line of the growth part represents the fit according to the power scaling relation $w \sim \phi^\beta$, while the dashed line indicates the trend of the data at very high doses.

Fig. 7. The plot of the correlation length ξ versus ion dose ϕ ; the fitting line indicates the slope yielding the value of z .

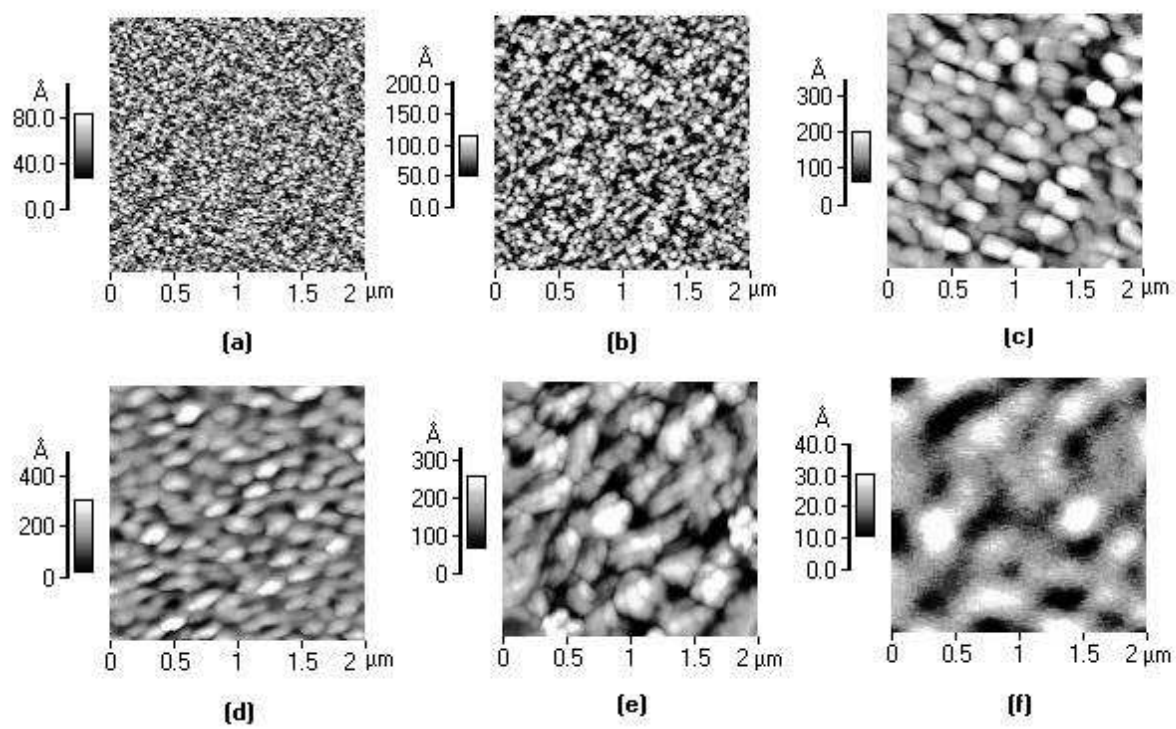
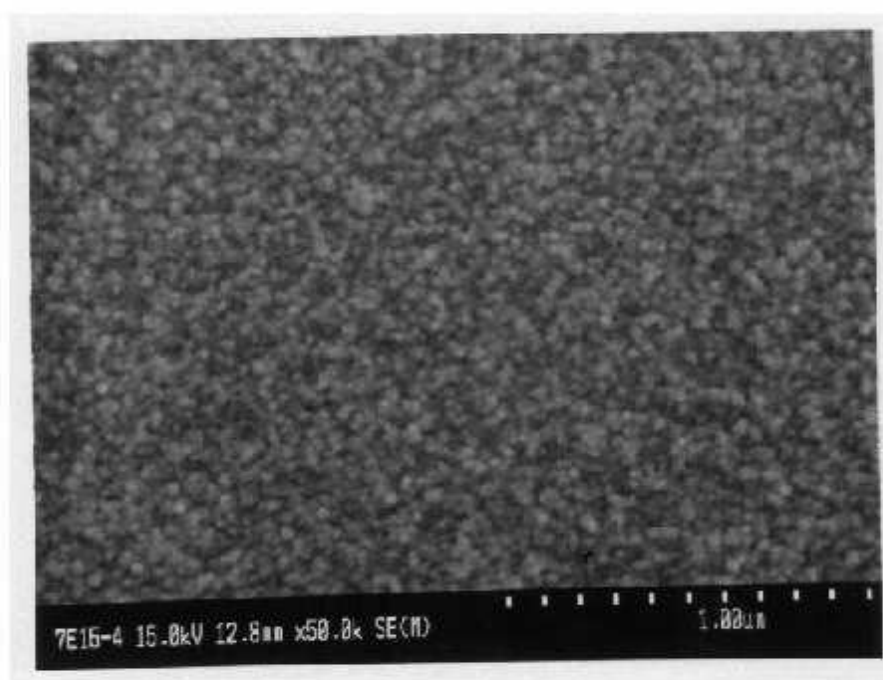
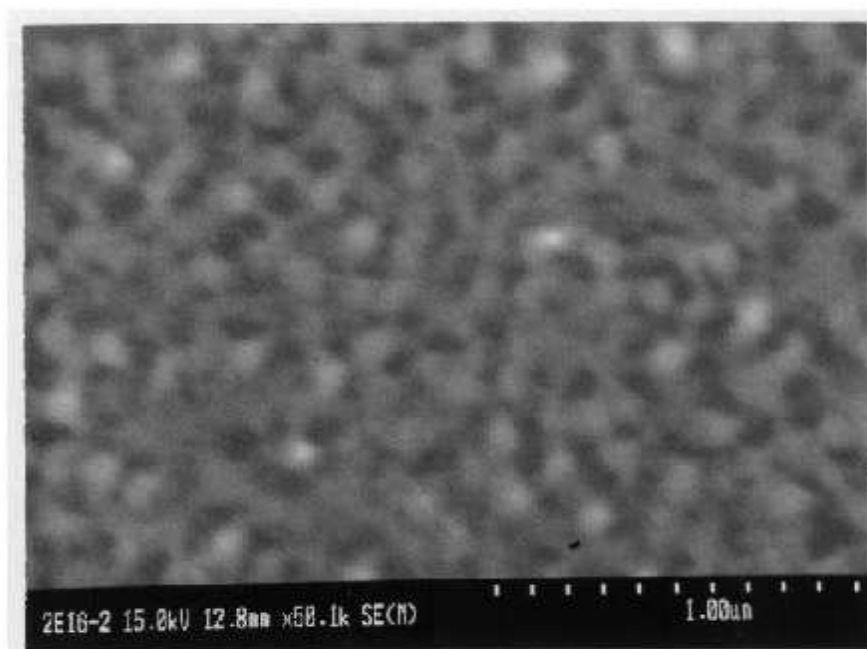


Fig. 1



(a)



(b)

Fig. 2

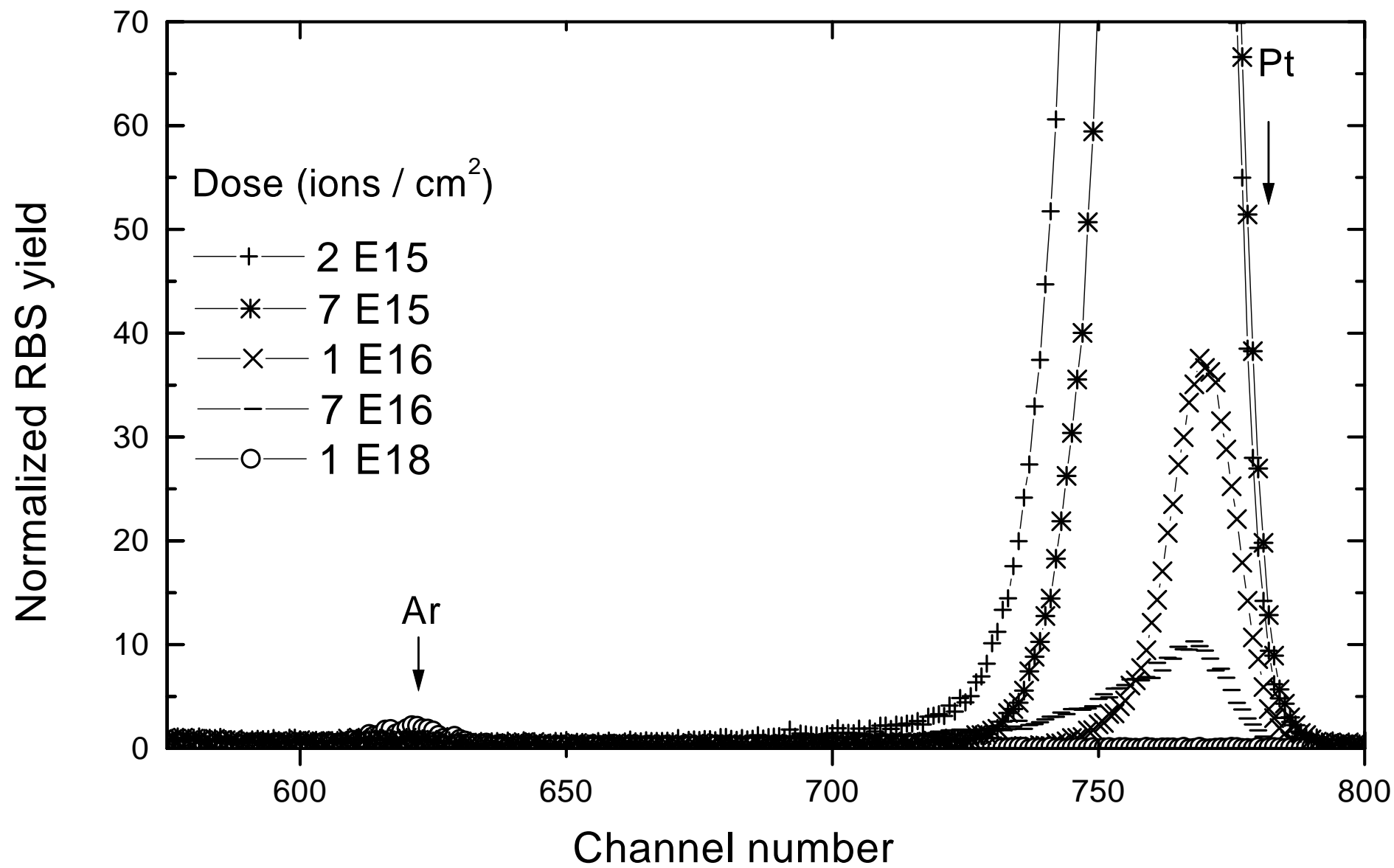


Fig. 3

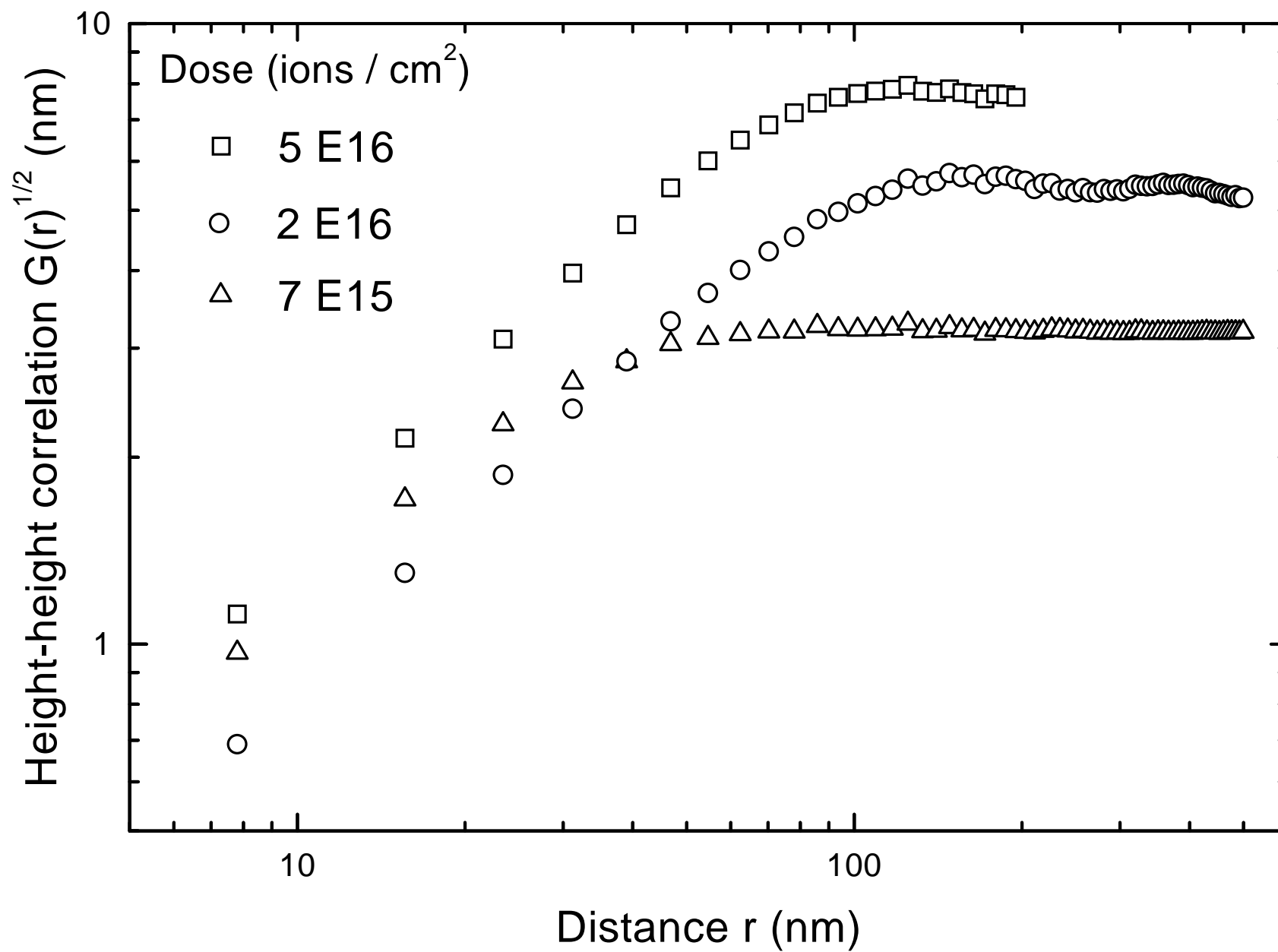


Fig. 4

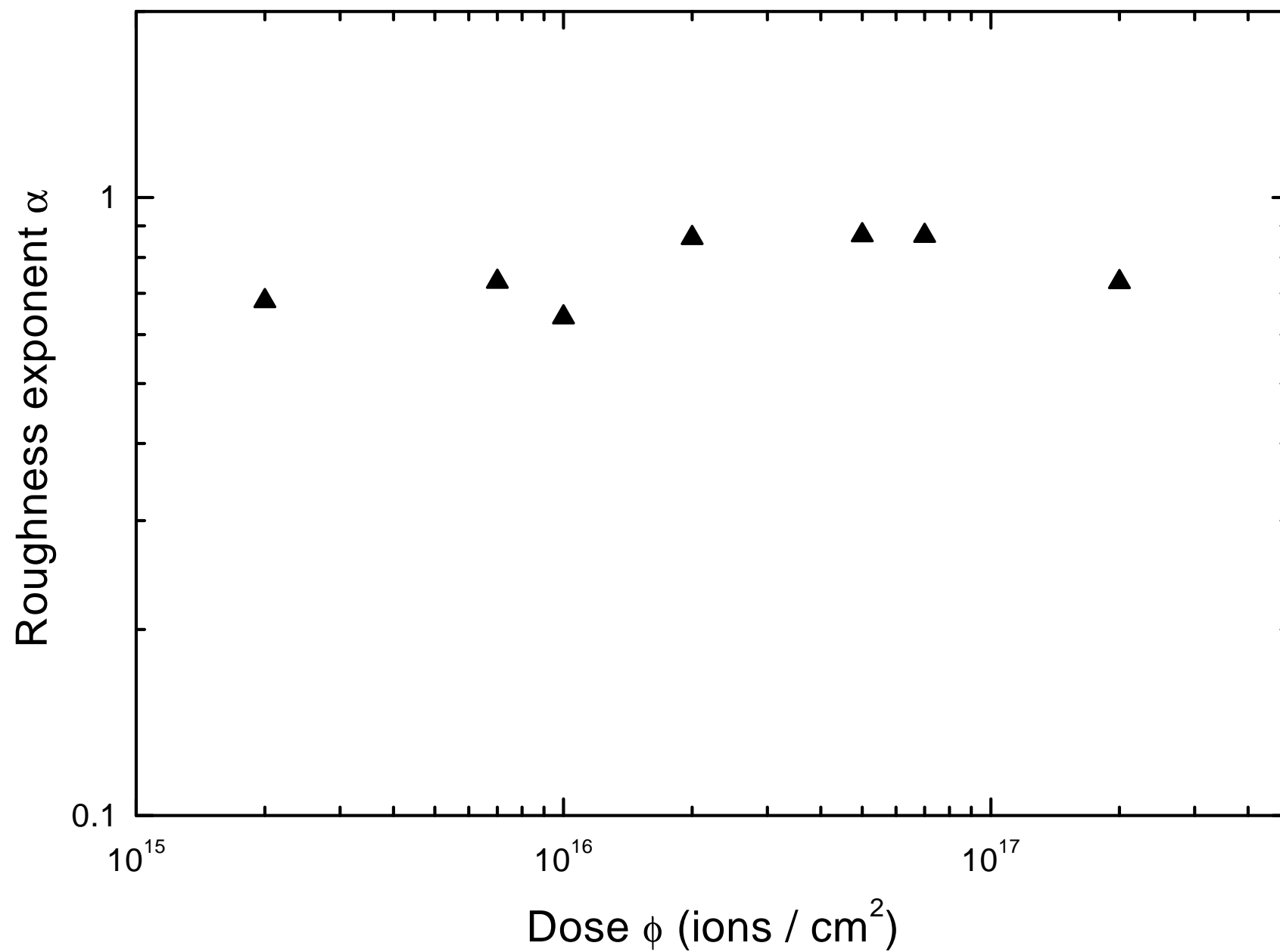


Fig. 5

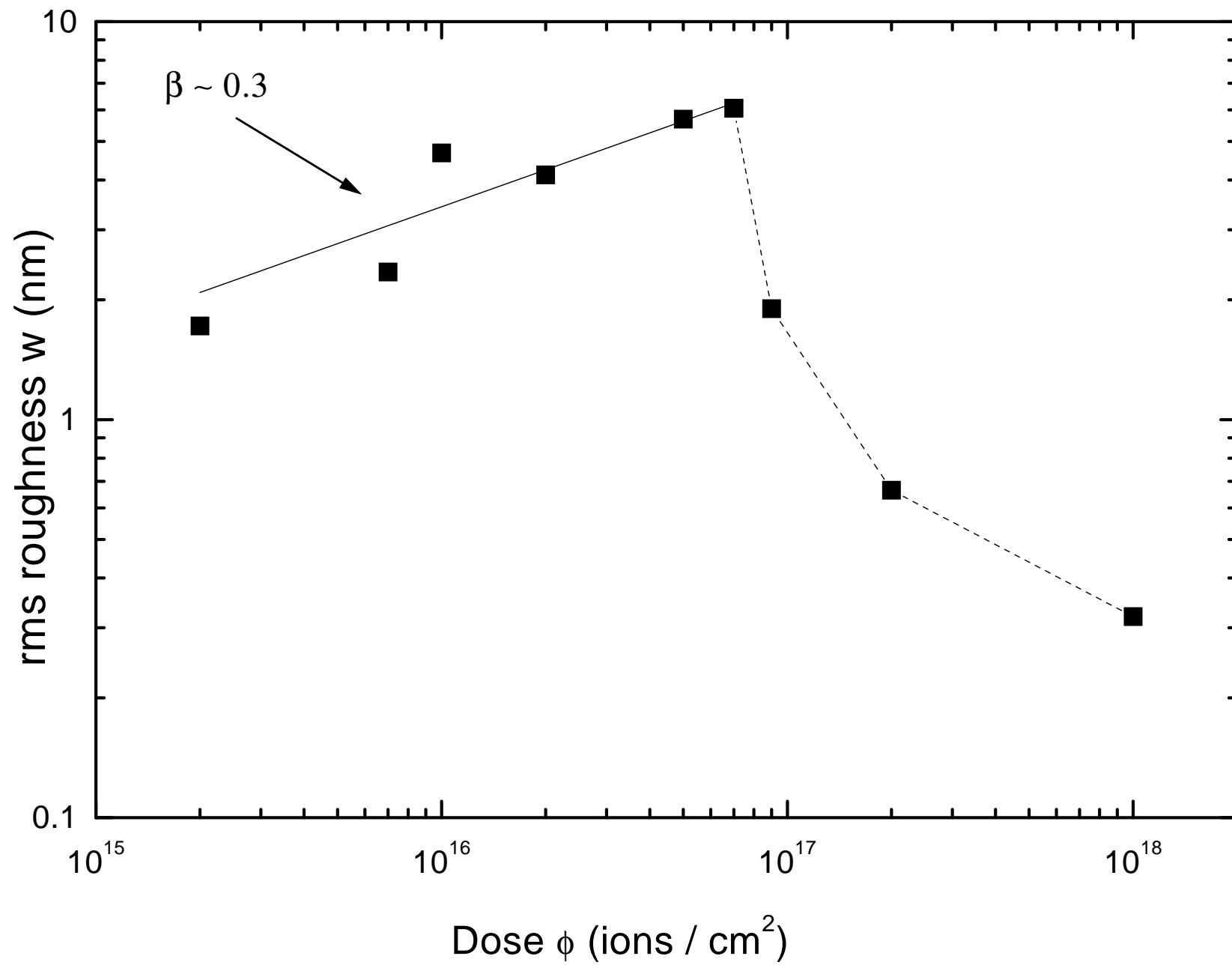


Fig. 6

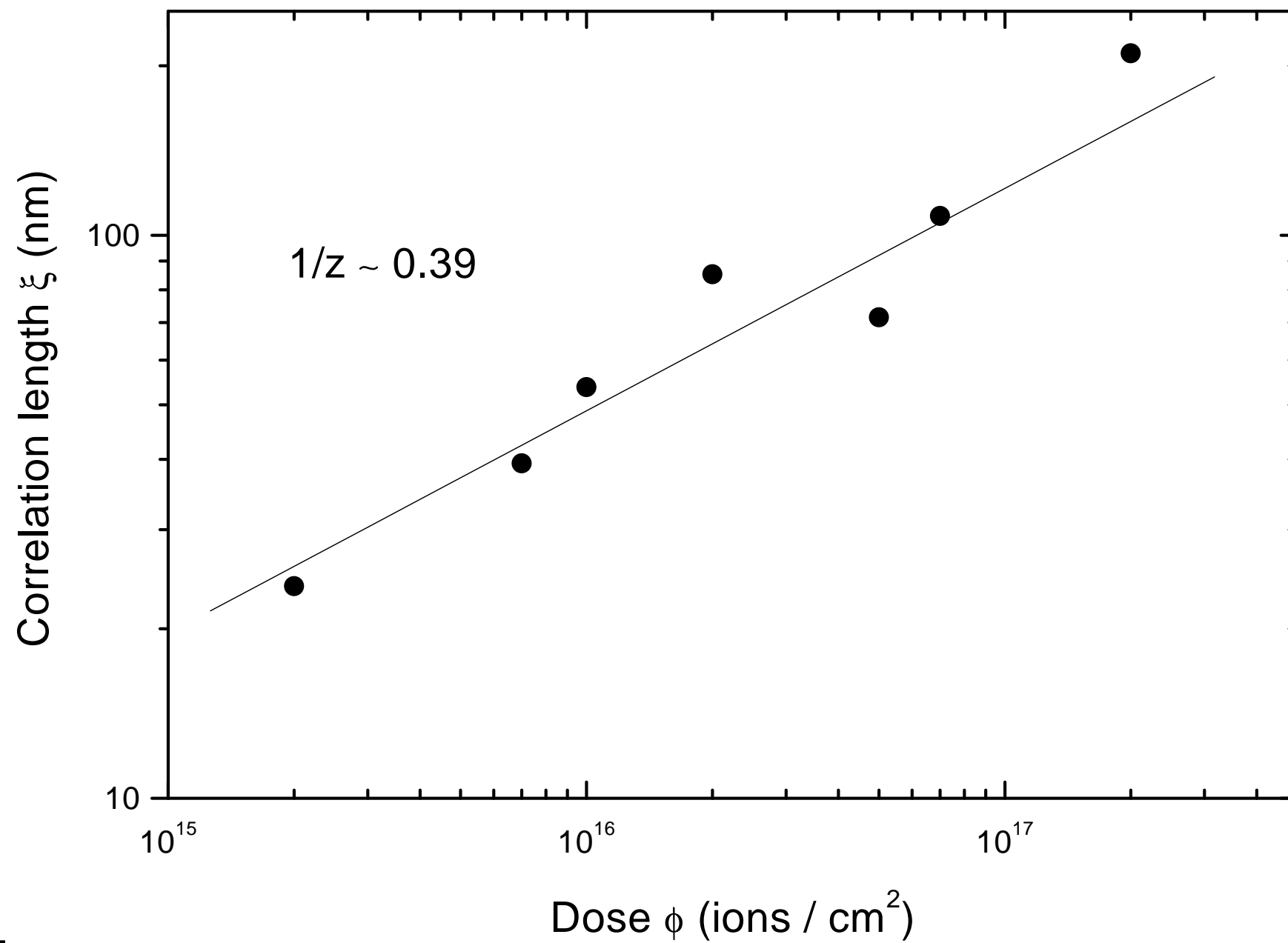


Fig. 7